Available online at www.sciencedirect.com

ScienceDirect

journal homepage: www.elsevier.com/locate/he

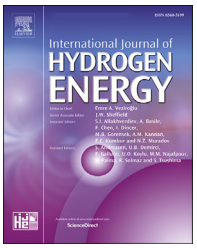

A comparative study of molybdenum phosphide catalyst for partial oxidation and dry reforming of methane

Yanzhao Cui [a], Qingyou Liu [b], Zhiwei Yao [a,*], Binlin Dou [c,**], Yan Shi [a], Yue Sun [a]

[a] Department of Petrochemical Engineering, College of Chemistry, Chemical Engineering and Environmental Engineering, Liaoning Shihua University, Fushun, 113001, PR China

[b] Key Laboratory of High-temperature and High-pressure Study of the Earth's Interior, Institute of Geochemistry, Chinese Academy of Sciences, Guiyang, 550081, PR China

[c] School of Energy and Power Engineering, University of Shanghai for Science and Technology, Shanghai, 200093, PR China

ARTICLE INFO

Article history:
Received 9 January 2019
Received in revised form
2 March 2019
Accepted 21 March 2019
Available online 10 April 2019

Keywords:
Molybdenum phosphide
Partial oxidation of methane
dry reforming of methane
Redox cycle
Catalytic stability

ABSTRACT

Molybdenum phosphide (MoP) was firstly used as a catalyst for partial oxidation of methane (POM) and its catalytic performance for POM was compared with that for dry reforming of methane (DRM). It was found that the MoP phase was the dominant active site in POM and DRM reactions, and the activity would gradually decrease when more and more MoP was converted to Mo_2C phase (non-dominant active site) and then rapid deactivation would occur due to bulk oxidation of catalyst. The redox type mechanism over MoP catalyst was vitally important to keep its structure reasonably well during methane reforming reactions. The MoP catalyst revealed a higher catalytic stability in POM than in DRM, attributing to the higher H_2 yield obtained in POM, which can promote and maintain the redox cycle of catalyst.

Introduction

Due to the fact that transition metal phosphides show unique catalytic activities similar to those of noble metal-based catalysts, they have attracted considerable attention in these twenty years and have been regarded as substitutes for noble metal catalysts in various catalysis fields [1,2]. To data, the metal phosphide-catalyzed reactions mainly focus on the hydrogen-involved thermocatalytic reactions (e.g. hydrogenation and hydrotreating [3,4] and N_2H_4 decomposition [5–7]), and the oxygen-involved electrocatalytic reactions [8,9], such as hydrogen evolution reaction (HER) [10–14], oxygen reduction reaction (ORR) [15,16] and oxygen evolution reaction (OER) [17,18]. However, the phosphide catalysts have received far less attention in the oxygen-involved thermocatalytic

* Corresponding author.
** Corresponding author.
E-mail addresses: mezhiwei@163.com (Z. Yao), bldou@usst.edu.cn (B. Dou).
https://doi.org/10.1016/j.ijhydene.2019.03.170

reactions. In our previous study, the phosphides of Mo, W, Fe, Co and Ni were used as catalysts for NO dissociation and their activities ranked in the order of $Fe_2P > Co_2P > MoP > WP > Ni_2P$. Unfortunately, the phosphide catalyst deactivation was inevitable due to surface oxidation by NO [19,20]. Subsequently, we have found that oxygen species generated from NO dissociation on phosphide surface can be removed efficiently by H_2 or CO, and thus the catalyst can retain the active phosphide phase in the NO/CO or NO/H_2 reaction [19,20]. Very recently, MoP and WP phosphides have been used as new catalysts in dry methane reforming (DRM, $CH_4+CO_2 = 2CO+2H_2$ (1)) [21,22]. Note that the catalytic stability of MoP was found to be much higher than that of bimetallic Ni/β-Mo_2C (well known to be an efficient non-noble metal catalyst for DRM) [22].

H_2 production from thermocatalytic reactions has been considered as the most promising technology, and some new approaches are also being developed for low-cost and high-efficiency [23,24]. In order to further develop phosphide catalysts in the oxygen-involved thermocatalytic reactions, in this study the MoP phosphide was firstly used as a catalyst in partial oxidation of methane (POM, $CH_4+1/2O_2 = CO+2H_2$ (2)) and its catalyst performance was compared with that in DRM.

Experimental

Catalyst preparation

The MoP catalyst was prepared by conventional H_2-temperature programmed reduction method, as previously described by Wang et al. [25]. Firstly, the oxidic precursor was prepared from aqueous solutions of $(NH_4)_6Mo_7O_{24}\cdot 4H_2O$ mixed with $(NH_4)_2HPO_4$ at a Mo:P mole ratio of 1:1. The mixture was stirred at room temperature (RT) for 1 h, and then dried overnight at 110 °C and the resultant solid was calcined at 500 °C for 3 h in air. Secondly, the oxidic precursor was reduced to MoP by H_2. The oxidic precursor was placed in a micro-reactor with an inner diameter of 10 mm and a flow of pure H_2 (150 ml min^{-1}) was introduced into the system. The temperature was increased from RT to 300 °C over a period of 30 min followed by a rise in temperature from 300 to 650 °C at a rate of 1 °C min^{-1}. The temperature was then kept at 650 °C for 2 h before cooling to RT in a H_2 flow. Finally, the material was passivated in 1%O_2/Ar for 12 h before it was exposed to air.

Catalyst characterization

X-ray diffraction (XRD) was conducted by an X-ray diffractometer (X'Pert Pro MPD) equipped with a Cu Kα source. X-ray photoelectron spectroscopy (XPS) was performed using a Kratos Axis ultra (DLD) equipped with Al Kα X-ray source. Charging effects were corrected according to adventitious carbon (284.6 eV) referencing. Raman spectroscopy was carried out using a Horrba/Jobin-Yvon LABRAM-HR spectrometer with the 632.8 nm line of a helium-neon laser as excitation source.

Catalyst performance tests

Catalytic activities of MoP for POM and DRM were evaluated in a micro-reactor with an inner diameter of 10 mm at atmospheric pressure. Prior to the reaction, the sample was preheated with H_2 to 850 °C and then further cooled or heated to a given reaction temperature (750–950 °C) under an Ar flow. Then two kinds of gas mixtures: (i) CH_4-O_2 and (ii) CH_4-CO_2 with mole ratios of 2:1 and 1:1, respectively, were separately allowed to pass through the catalyst (0.1 g, 60–80 mesh) at a flow rate of 45 ml min^{-1}. The weight hourly space velocity (WHSV) was 27000 $cm^3\ g^{-1}\ h^{-1}$. In addition, Carbon dioxide/oxygen temperature-programmed oxidation (CO_2/O_2-TPO) studies were performed using a flow of 2%CO_2 (or O_2) in Ar (50 ml min^{-1}). Prior to the reaction, the sample was heated to 850 °C under Ar (50 ml min^{-1}), followed by cooling to RT under Ar, and then was heated under the reactant gas from RT to 850 °C at a rate of 10 °C min^{-1}. The exit gas stream from the reactor passed through a cold trap to remove water. The flow rates were measured with a soap bubble flow meter. The gas-phase products were analyzed by on-line gas chromatography (GC) equipped with a thermal conductivity dectector and a TDX-01 (60–80 mesh) packed column (300 mm × 2 mm i.d.). The carrier gas and reference gas were Ar (99.999%) and the column flow rate was 30 ml min^{-1}. The column temperature and detector temperature were operated at 70 and 100 °C, respectively. Reference data and pure component injections were used to indentify the major peaks, and response factors for the products and reactants were determined and taken into account in the calculation of the conversion and product distribution. The conversions of CH_4, O_2 and CO_2, and selectivity of H_2 were defined respectively as follows:

$$CH_4\ \text{conversion} = \frac{\text{moles of } CH_4 \text{ converted}}{\text{moles of } CH_4 \text{ introduced}} \times 100\%\ ;$$

$$O_2\ \text{conversion} = \frac{\text{moles of } O_2 \text{ converted}}{\text{moles of } O_2 \text{ introduced}} \times 100\%\ ;$$

$$CO_2\ \text{conversion} = \frac{\text{moles of } CO_2 \text{ converted}}{\text{moles of } CO_2 \text{ introduced}} \times 100\%\ ;$$

$$H_2\ \text{selectivity} = \frac{\text{moles of } H_2 \text{ produced}}{2 \times \text{moles of } CH_4 \text{ converted}} \times 100\%\ .$$

Results and discussion

Fig. 1 shows the temperature dependence of catalytic performance over MoP catalyst for POM and DRM reactions. It can be observed from Fig. 1 that the catalytic performance of MoP was greatly dependent on temperature. As for the POM, the CH_4 conversion and H_2 selectivity increased from 48 to 88% and 43–81%, respectively, in a linear fashion with temperature, but the O_2 conversion was always 100% in the whole temperature range (750–900 °C). In addition, the conversion of O_2 was higher than that of CH_4, probably due to the MoP-contained redox type mechanism (as discussed later) and the side reaction of methane combustion occurred in POM [26]. As for the DRM, the CH_4 conversion and CO_2 conversion increased from 40 to 73% and 53–86%, respectively, with the increase of temperature, but the H_2 selectivity showed a "volcano" shape with the highest value (77%) at 850 °C. After

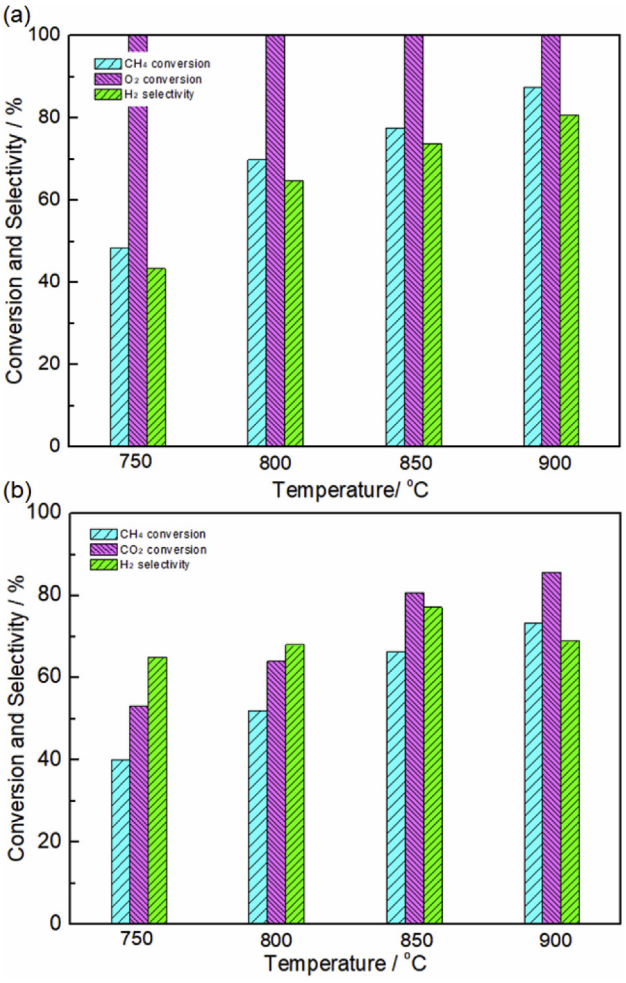

Fig. 1 – Dependence of catalytic performance on temperature over the MoP catalyst for (a) POM and (b) DRM. Reaction conditions: CH_4:O_2 = 2:1, CH_4:CO_2 = 1:1, WHSV = 27000 cm^3 g^{-1} h^{-1}, reaction pressure = 1 atm, reaction time = 2 h.

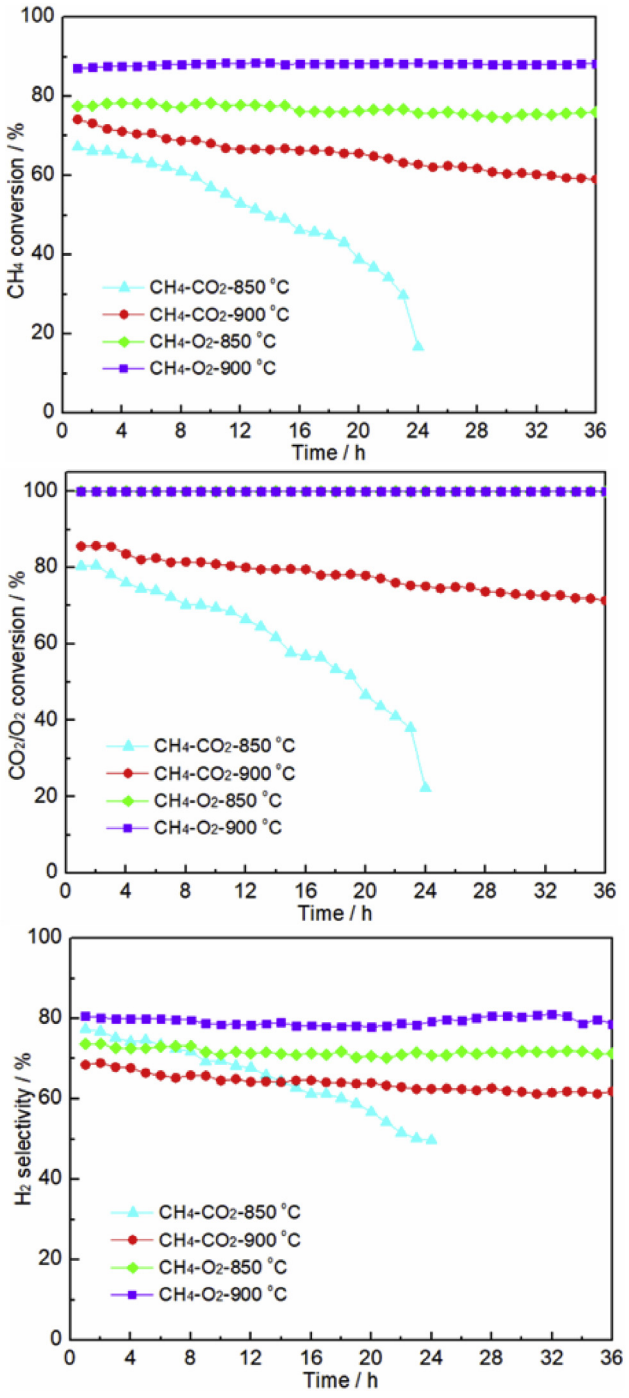

Fig. 2 – Catalytic stability of MoP catalyst for POM and DRM. Reaction conditions: CH_4:O_2 = 2:1, CH_4:CO_2 = 1:1, WHSV = 27000 cm^3 g^{-1} h^{-1}, reaction pressure = 1 atm, reaction temperature = 850 or 900 °C.

making the comparison, it was found that the MoP showed a higher catalytic activity in POM than in DRM.

Subsequently, the catalytic stability of MoP catalyst for POM and DRM reactions at high temperatures was further investigated and the results are shown in Fig. 2. Clearly, the MoP catalyst showed a stable activity through out the test period of 36 h in POM reaction, no matter whether it was at 850 or 900 °C. However, the activity of MoP decreased at a low rate with time in DRM reaction, and even the catalyst suffered from gradual deactivation at 850 °C.

Coking and structural change were usually reported to be the main reasons for the decrease of catalyst activity in methane reforming reactions [27]. In order to further investigate the reason why the catalytic stability of MoP in POM was higher than that in DRM, the fresh and used catalysts were characterized by XRD, XPS and Raman spectroscopy. It can be seen from Fig. 3 that in the case of the MoP samples functioned in POM at 850 and 900 °C, there was a series of weak peaks of Mo_2C coexisting with those of MoP. The results indicated that a very small portion of MoP was converted to Mo_2C during high-temperature POM. Compared with the XRD patterns of the used samples in POM, the XRD patterns of the used samples in DRM at 850 and 900 °C showed an increase in intensity of Mo_2C peaks, and more notably, a new set of peaks due to MoO_2 was observed on the used sample at 850 °C. The results indicated that more MoP was lost in DRM at 850 and 900 °C, especially at 850 °C.

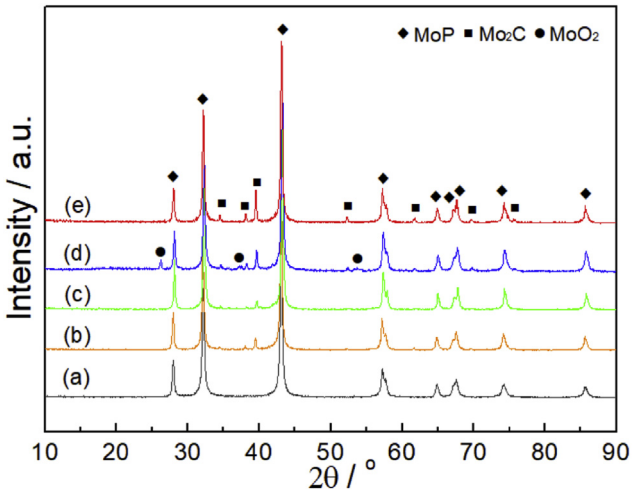

Fig. 3 – XRD patterns of fresh MoP (a), used MoP in POM at 850 °C (b), and 900 °C (c), and used MoP in DRM at 850 °C (d) and 900 °C (e).

Fig. 4 shows the XPS spectra of Mo 3d and P 2p for the fresh MoP catalyst and used MoP catalysts in POM and DRM at 850 °C. The Mo 3d and P 2p doublet peaks should have splittings of ~3.2 and ~0.9 eV, respectively. The Mo $3d_{5/2}$ to Mo $3d_{3/2}$ and P $2p_{3/2}$ to P $2p_{1/2}$ intensity ratios were 3/2 and 2/1, respectively. On the basis of deconvolution, the distribution of molybdenum and phosphorus oxidation states, and the ratios of surface Mo species in MoP to total Mo species ($Mo^{\delta+}/(Mo^{\delta+}+Mo^{4+}+Mo^{6+})$, designated as R) are estimated and summarized in Table 1. It can be seen from Fig. 4 and Table 1 that there were three Mo species and two P species on the fresh and used samples. The Mo $3d_{5/2}$ binding energies of 228.0–228.2, 228.8–229.0 and 232.1–232.3 eV were attributed to $Mo^{\delta+}$, Mo^{4+} and Mo^{6+} species, respectively, and the P $2p_{3/2}$ binding energies of 129.3–129.5 and 133.4–133.5 eV were identified as $P^{\delta-}$ and P^{5+} species, respectively [28,29]. In view of the fact that the XRD results (Fig. 3) confirmed the formation of Mo_2C phase in the two used samples, there was the presence of Mo species in the form of Mo_2C on the catalyst surfaces. Nevertheless, it was impossible to distinguish between Mo^{2+} in Mo_2C (228.1–228.6 eV) [30,31] and $Mo^{\delta+}$ in MoP (228.0–228.4 eV) [32–34] by XPS because their Mo $3d_{5/2}$ binding energy values were close to each other. It was worthy to note that the R (0.38) of used MoP in POM was close to that (0.40) of fresh MoP, however, the R (0.26) of the used MoP in DRM was far away from that of fresh MoP. Indeed, the theoretical values of R for used MoP samples should be lower than the actual estimated values owing to the existence of Mo_2C species. The results suggested that the MoP catalyst can keep its structure relatively stable at 850 °C in POM but it suffered from bulk oxidation at 850 °C in DRM. These findings were in good consistent with the XRD observation in Fig. 3.

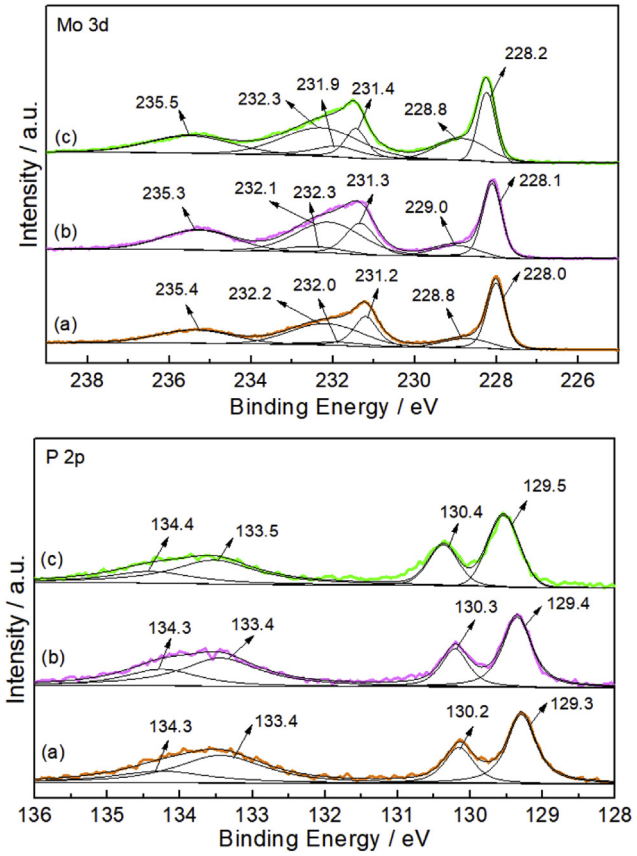

Fig. 4 – Deconvolution of Mo 3d and P 2p XPS spectra of fresh MoP (a), used MoP in POM at 850 °C for 36 h (b) and used MoP in DRM at 850 °C for 24 h (c).

It was suggested that the single metal Mo_2C-based catalysts were also catalytically active in POM and DRM at atmospheric pressure but they would suffer from rapid deactivation due to bulk oxidation [25,35–38]. Therefore, it was reasonable to obtain these deductions: (i) the MoP phase was the dominant active site in POM and DRM reactions (ii) the activity (e.g. in DRM at 900 °C); would gradually decrease when more and more MoP was converted to Mo_2C phase (non-dominant active site) (iii) rapid deactivation (e.g. in DRM at 850 °C); occurred due to bulk oxidation of catalyst. In addition, the Raman results (Fig. S1 in supporting information) confirmed that no obvious peaks were observed for graphite (~1577 cm^{-1}) or amorphous carbon species (~1345 cm^{-1}) [24], indicating no carbon deposition formed on the MoP catalyst during POM and DRM reactions. Thus, it can be concluded that the decrease in the activity of MoP catalyst was indeed due to structural change (MoP→Mo_2C or MoO_2) rather than coking.

It was reported that the redox type mechanism over MoP catalyst was vitally important to keep its structure reasonably well during DRM [22]. And the redox cycle route was further proposed based on our previous studys [22,39] as follows.

$$MoP \underset{CH_4,H_2}{\overset{CO_2}{\rightleftarrows}} MOP_xO_y \quad (3)$$

$$MoP + CO_2 \rightarrow MoO_2 + CO + PO_x \quad (4)$$

$$MoO_2 + PO_x + H_2 \rightarrow MoP + H_2O \quad (5)$$

$$2MoO_2 + 5CH_4 = Mo_2C + 4CO + 10H_2 \quad (6)$$

$$Mo_2C + 5CO_2 = 2MoO_2 + 6CO \quad (7)$$

Table 1 – XPS results for fresh MoP, used MoP in POM at 850 °C for 36 h and used MoP in DRM at 850 °C for 24 h.

Sample	Binding energy (eV)					R
	Mo $3d_{3/2}$/Mo $3d_{5/2}$			P $2p_{1/2}$/P $2p_{3/2}$		
	$Mo^{\delta+}$	Mo^{4+}	Mo^{6+}	$P^{\delta-}$	P^{5+}	
Fresh MoP	231.2/228.0	232.0/228.8	235.4/232.2	130.2/129.3	134.3/133.4	0.40
Used MoP in POM	231.3/228.1	232.3/229.0	235.3/232.1	130.3/129.4	134.3/133.4	0.38
Used MoP in DRM	231.4/228.2	231.9/228.8	235.5/232.3	130.4/129.5	134.4/133.5	0.26

$R = Mo^{\delta+}/(Mo^{\delta+}+Mo^{4+}+Mo^{6+})$.

Initially the MoP catalyst suffered from oxidation during DRM and then the oxidation products, MoP_xO_y and MoO_2, were in-situ reduced by CH_4 or H_2 to produce MoP and Mo_2C. The XRD results (see Fig. 3) only proved the existence of Mo_2C and MoO_2 phases on the used catalysts because the MoP_xO_y phase was usually in the form of amorphous state [22]. Clearly, this redox type mechanism over MoP should also exist in POM using O_2 as oxidant instead of CO_2. Our previous study had proved that MoP can be oxidized by O_2 to Mo oxide-phosphate [40]. Notably, the TPO results (Fig. 5) indicated that the amount of O_2 consumption increased more quickly than that of CO_2 consumption when the temperature was above 350 °C. Therefore, it can be deduced that the MoP was oxidized more easily by O_2 than by CO_2. In other words, the oxidation rate of MoP in POM was higher than that in DRM. However, it was indicated from Fig. 3 that the MoP showed higher structural stability in POM than in DRM. It was reasonable to deduce that the reduction rate of MoP_xO_y/MoO_2 in POM should be much higher than that in DRM. In order to confirm the deduction, the H_2 yield rate estimated from Fig. 1 was shown in Fig. 6. It was clear that the POM produced much more H_2 than DRM above 800 °C, which can lead to the faster reduction of Mo-containing species in POM. Thus, it was possible that the redox cycle of catalyst was established more easily in POM than in DRM and then the bulk oxidation of catalyst can be avoided.

In view of the effect of H_2 content in effluent gas on the catalytic stability of MoP for methane reforming reactions, the catalytic stability of MoP was further investigated for the DRM with added H_2 (see Fig. 7). By comparing Fig. 7 with Fig. 2, it was clear that the catalytic stability of MoP was indeed greatly enhanced after adding H_2 into DRM feed gas. Moreover, the XRD and XPS results for the used sample (see Figs. S2 an S3)

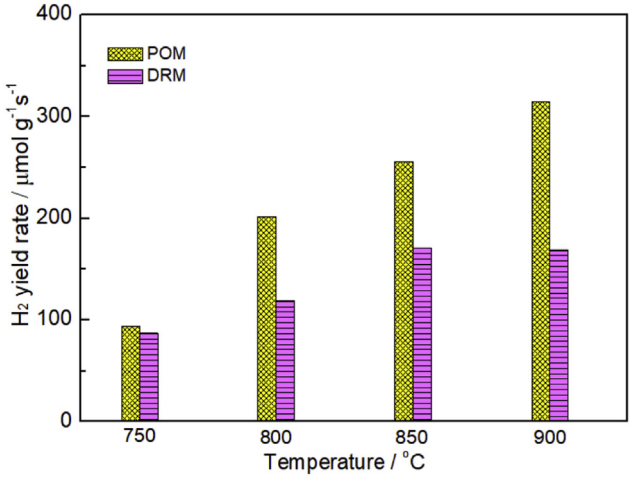

Fig. 6 – H_2 yield rate over the MoP catalyst for POM and DRM reactions. Reaction conditions: CH_4:O_2 = 2:1, CH_4:CO_2 = 1:1, WHSV = 27000 $cm^3\ g^{-1}\ h^{-1}$, reaction pressure = 1 atm, reaction time = 2 h.

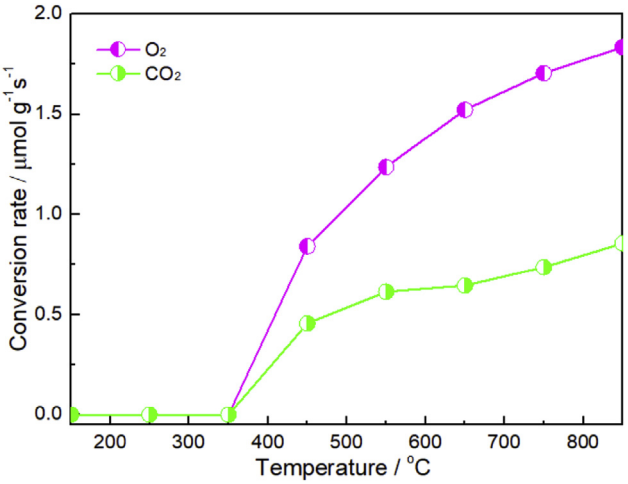

Fig. 5 – Conversion rates of O_2 and CO_2 obtained from O_2-TPO and CO_2-TPO studies.

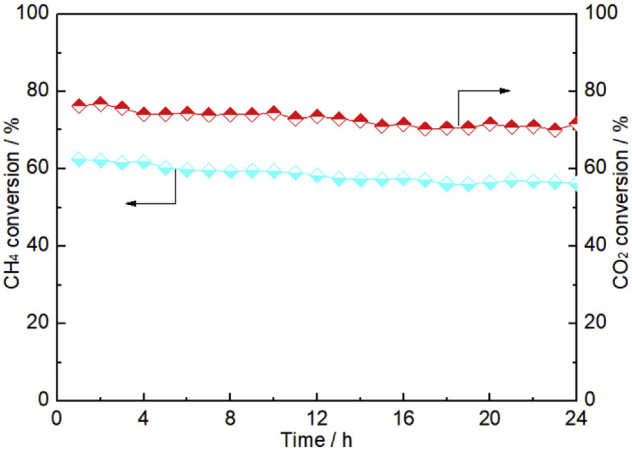

Fig. 7 – Catalytic stability of MoP catalyst for CH_4-CO_2-H_2 reaction. Reaction conditions: CH_4:CO_2:H_2 = 1:1:0.4, WHSV = 32400 $cm^3\ g^{-1}\ h^{-1}$, reaction pressure = 1 atm, reaction temperature = 850 °C.

proved that the addition of H_2 into DRM feed gas can avoid bulk oxidation of MoP catalyst. It can be therefore concluded that the MoP catalyst showed higher stability in POM than in DRM due to the higher H_2 yield obtained in POM, which was vital to maintain the redox cycle of MoP system in methane reforming reactions.

Conclusions

After MoP was used as a DRM catalyst, it was used as a POM catalyst for the first time in this work. It was found that the MoP was a more excellent catalyst in POM than in DRM in terms of both activity and stability. Higher catalytic stability shown in POM was attributed to the higher H_2 yield in effluent gas, which was beneficial to maintain the redox cycle of MoP system in methane reforming reactions. This study has developed a new oxygen-involved thermocatalytic reaction using MoP as a catalyst, and further studies on the redox behavior of the MoP catalyst in various oxygen-involved thermocatalytic reactions are highly desirable.

Acknowledgments

The work was supported by the National Natural Science Foundation of China (No. 21276253, 51876130, 51476022), the Liaoning Province Natural Science Foundation (No. 20180551272) and the Project of Liaoning Province Department of Education (No. L2017LZD003).

Appendix A. Supplementary data

Supplementary data to this article can be found online at https://doi.org/10.1016/j.ijhydene.2019.03.170.

REFERENCES

[1] Alexander A-M, Hargreaves JSJ. Alternative catalytic materials: carbides, nitrides, phosphides and amorphous boron alloys. Chem Soc Rev 2010;39:4388–401.
[2] Brock SL, Senevirathne K. Recent developments in synthetic approaches to transition metal phosphide nanoparticles for magnetic and catalytic applications. J Solid State Chem 2008;181:1552–9.
[3] Oyama ST, Gott T, Zhao H, Lee Y-K. Transition metal phosphide hydroprocessing catalysts: a review. Catal Today 2009;143:94–107.
[4] Oyama ST. Novel catalysts for advanced hydroprocessing: transition metal phosphides. J Catal 2003;216:343–52.
[5] Ding L, Shu Y, Wang A, Zheng M, Li L, Wang X, Zhang T. Preparation and catalytic performances of ternary phosphides NiCoP for hydrazine decomposition. Appl Catal A-Gen 2010;385:232–7.
[6] Cheng R, Shu Y, Zheng M, Li L, Sun J, Wang X, Zhang T. Molybdenum phosphide, a new hydrazine decomposition catalyst: microcalorimetry and FTIR studies. J Catal 2007;249:397–400.
[7] Zheng M, Shu Y, Sun J, Zhang T. Carbon-covered alumina: a superior support of noble metal-like catalysts for hydrazine decomposition. Catal Lett 2008;121:90–6.
[8] Lv Y, Wang X. Nonprecious metal phosphides as catalysts for hydrogen evolution, oxygen reduction and evolution reactions. Catal Sci Technol 2017;7:3676–91.
[9] Callejas JF, Read CG, Roske CW, Lewis NS. Schaak RE. Synthesis, characterization and properties of metal phosphide catalysts for the hydrogen-evolution reaction. Chem Mater 2016;28:6017–44.
[10] Zhang R, Wang X, Yu S, Wen T, Zhu X, Yang F, et al. Ternary $NiCo_2Px$ nanowires as pH-universal electrocatalysts for highly efficient hydrogen evolution reaction. Adv Mater 2017;29:1605502.
[11] Zhuang M, Ou X, Dou Y, Zhang L, Zhang Q, Wu R, et al. Polymer-embedded fabrication of Co_2P nanoparticles encapsulated in N, P-doped graphene for hydrogen generation. Nano Lett 2016;16:4691–8.
[12] Yang F, Zhao Y, Du Y, Chen Y, Cheng G, Chen S, et al. A monodisperse Rh_2P-based electrocatalyst for highly efficient and pH-universal hydrogen evolution reaction. Adv Energy Mater 2018;8:1703489.
[13] Yang F, Chen Y, Cheng G, Chen S, Luo W. Ultrathin nitrogen-doped carbon coated with CoP for efficient hydrogen evolution. ACS Catal 2017;7:3824–31.
[14] Du C, Yang L, Yang F, Cheng G, Luo W. Nest-like NiCoP for highly efficient overall water splitting. ACS Catal 2017;7:4131–7.
[15] Wu Z-S, Chen L, Liu J, Parvez K, Liang H, Shu J, et al. High performance electrocatalysts for oxygen reduction derived from cobalt porphyrin-based conjugated mesoporous polymers. Adv Mater 2014;26:1450–5.
[16] Vicky VTD, Zhang S, Edward BT, Rahul A, Li J, Su D, et al. Recent advances in chemical functionalization of nanoparticles with biomolecules for analytical applications. ACS Nano 2015;9:8108–15.
[17] Guan B, Yu L, Lou X. General synthesis of multishell mixed-metal oxyphosphide particles with enhanced electrocatalytic activity in the oxygen evolution reaction. Angew Chem Int Ed 2017;56:2386–9.
[18] He P, Yu X, Lou X. Carbon-incorporated nickel-cobalt mixed metal phosphide nanoboxes with enhanced electrocatalytic activity for oxygen evolution. Angew Chem Int Ed 2017;56:3897–900.
[19] Yao Z, Dong H, Shang Y. Catalytic activities of iron phosphide for NO dissociation and reduction with hydrogen. J Alloy Comp 2009;474:L10–3.
[20] Yao Z, Qiao X, Liu D, Shi Y, Zhao Y. Catalytic activities of transition metal phosphides for NO dissociation and reduction with CO. Chem Biochem Eng Q 2016;29:505–10.
[21] Yang C, Li X, Yang Y, Yang X, Yang A. Study on a new catalyst tungsten phosphide for the carbon dioxide reforming of methane and its preparation conditions. Asian J Chem 2013;25:3601–4.
[22] Yao Z, Luan F, Sun Y, Jiang B, Song J, Wang H. Molybdenum phosphide as a novel and stable catalyst for dry reforming of methane. Catal Sci Technol 2016;6:7996–8004.
[23] Dou B, Zhang H, Cui G, Wang Z, Jiang B, Wang K, et al. Hydrogen production and reduction of Ni-based oxygen carriers during chemical looping steam reforming of ethanol in a fixed-bed reactor. Int J Hydrogen Energy 2017;42:26217–30.
[24] Dou B, Zhang H, Cui G, Wang Z, Jiang B, Wang K, et al. Hydrogen production by sorption-enhanced chemical looping steam reforming of ethanol in an alternating fixed-bed reactor: sorbent to catalyst ratio dependencies. Energy Convers Manag 2018;155:243–52.

[25] Wang X, Clark P, Oyama ST. Oyama, Synthesis, characterization, and hydrotreating activity of several iron group transition metal phosphides. J Catal 2002;208:321–31.
[26] Xiao T-C, Hanif A, York APE, Green MLH. Methane partial oxidation to synthesis gas over bimetallic cobalt/tungsten carbide catalysts and integration with a Mn substituted hexaaluminate combustion catalyst. Catal Today 2009;147:196–202.
[27] Yao Z, Jiang J, Zhao Y, Luan F, Zhu J, Shi Y. Insights into the deactivation mechanism of metal carbide catalysts for dry reforming of methane via comparison of nickel-modified molybdenum and tungsten carbides. RSC Adv 2016;6:19944–51.
[28] Xiao P, Sk MA, Thia L, Ge X, Lim RJ, Wang J-Y, et al. Molybdenum phosphide as an efficient electrocatalyst for the hydrogen evolution reaction. Energy Environ Sci 2014;7:2624–9.
[29] Guo L, Zhao Y, Yao Z. Mechanical mixtures of metal oxides and phosphorus pentoxide as novel precursors for the synthesis of transition-metal phosphides. Dalton Trans 2016;45:1225–32.
[30] Shi C, Zhang A, Li X, Zhang S, Zhu A, Ma Y, et al. Ni-modified Mo_2C catalysts for methane dry reforming. Appl Catal A-Gen 2012;431:164–70.
[31] Zhao Y, Yao Z, Shi Y, Qiao X, Wang G, Wang H, et al. A novel approach to the synthesis of bulk and supported β-Mo 2 C using dimethyl ether as a carbon source. New J Chem 2015;39:4901–8.
[32] Abu II , Smith KJ. The effect of cobalt addition to bulk MoP and Ni_2P catalysts for the hydrodesulfurization of 4, 6-dimethyldibenzothiophene. J Catal 2006;241:356–66.
[33] Chen J, Yang Y, Shi H, Li M, Chu Y, Pan Z, et al. Regulating product distribution in deoxygenation of methyl laurate on silica-supported Ni-Mo phosphides: effect of Ni/Mo ratio. Fuel 2014;129:1–10.
[34] Yao Z, Li M, Wang X, Qiao X, Zhu J, Zhao Y, et al. A novel synthetic route to transition metal phosphide nanoparticles. Dalton Trans 2015;44:5503–9.
[35] Xiao T-C, Hanif A, York APE, Nishizaka Y, Green MLH. Study on the mechanism of partial oxidation of methane to synthesis gas over molybdenum carbide catalyst. Phys Chem Chem Phys 2002;4:4549–54.
[36] Zhu Q, Yang J, Wang J, J S, Wang H. Investigation on the performance of supported molybdenum carbide for the partial oxidation of methane. J Nat Gas Chem 2003;12:23–30.
[37] Gao H, Yao Z, Shi Y, Jia R, Liang P, Sun Y, et al. Simple and large-scale synthesis of β-phase molybdenum carbides as highly stable catalysts for dry reforming of methane. Inorg Chem Front 2018;5:90–9.
[38] Gao H, Yao Z, Shi Y, Wang S. Improvement of the catalytic stability of molybdenum carbide via encapsulation within carbon nanotubes in dry methane reforming. Catal Sci Technol 2018;8:697–701.
[39] Guo L, Zhao Y, Yao Z. Mechanical mixtures of metal oxides and phosphorus pentoxide as novel precursors for the synthesis of transition-metal phosphides. Dalton Trans 2016;45:1225–32.
[40] Yao Z, Lai Z, Zhang X, Peng F, Yu H, Wang H. Structural stability and mutual transformations of molybdenum carbide, nitride and phosphide. Mater Res Bull 2011;46:1938–41.